Low-wave-number Raman scattering from CdS$_x$Se$_{1-x}$ quantum dots embedded in a glass matrix

M. Ivanda,[1,2] K. Babocsi,[1] C. Dem,[1] M. Schmitt,[1] M. Montagna,[3] and W. Kiefer[1,*]

[1]*Institut für Physikalische Chemie, Universität Würzburg, Am Hubland, D-97074 Würzburg, Germany*
[2]*Ruđer Bošković Institute, P.O. Box 180, 10002 Zagreb, Croatia*
[3]*Instituto Nationale di Fisica della Materia, Dipartimento di Fisica, Università di Trento, I-38050 Povo, Trento, Italy*

The Raman scattering on acoustical phonons from CdS$_x$Se$_{1-x}$ quantum dots in a glass matrix were investigated for in- and off-resonance conditions. By a comparison with a model calculation, the off-resonance scattering showed that the homogeneous broadening mainly contributes to the spectral width of the acoustical vibrational modes. The contribution of inhomogeneous broadening is 30% of the symmetric mode linewidth. For photodarkened samples measured under resonance conditions we showed by comparing the experimental results with the calculations that the ground levels for resonant particle excitation are the trap states filled with the carriers by a photodarkening process. The determined trap energies are in the range of 1–1.5 eV.

I. INTRODUCTION

A semiconductor-doped glass consists of nanosized crystals of CdS$_x$Se$_{1-x}$ ($0 < x < 1$) embedded in a glass host. This kind of glass is one example of the many zero-dimensional quantum-confined electronic systems. The properties of such systems are related to the confinement of the (quasi)particles (electrons, holes, excitons, phonons, etc.) down to radii less than 10 nm. The increased interest for this material started with the discovery of its saturable absorption, which makes it promising for using as a Q-switching element in lasers.[1] The large nonlinear properties[2] as well as the fast response times[3] of these materials make them interesting for applications in waveguides,[4] optical switches,[5] or bistable resonators.[3]

The electron-phonon coupling in these materials is of prime importance because its strength increases with decreasing crystallite size.[6] Compared to the electronic states, there is only little information available on the vibrational modes of nanocrystals. In addition, one major requirement for an application of these materials in the field of nonlinear optics is to have an accurate knowledge of the particle size and size distribution. Raman scattering is one of the best nondestructive techniques to obtain information about the structure and the electronic and vibrational states in such a confined system. It is sensitive to the surface conditions, the mean particle size, and the width of the particle size distribution of a nanoparticle system. The investigation of the low-wave-number Raman scattering (LWR) related to the elastic vibrations of small particles[7] have been also applied to the CdS$_x$Se$_{1-x}$ semiconductor nanoparticles to determine their size[8–13] and the influence of the excitation radiation frequency on the shape and intensity of the LWR acoustical bands.[14]

In this paper we present a systematic study of the LWR scattering of confined acoustical modes of CdS$_x$Se$_{1-x}$ quantum dots (QD's) of various size recorded under resonance and off-resonance conditions. The purpose of this article is to present a comparative study between these scattering conditions. For the off-resonant scattering we have estimated the contribution of the homogeneous broadening on the symmet-

ric mode. In the resonant scattering regime we have analyzed which particles were involved in the scattering process and how the photodarkening process influences the resonant Raman scattering.

II. EXPERIMENT

Commercially available Schott filter glasses with different concentrations of CdS$_x$Se$_{1-x}$ quantum dots of different sizes—in particular, GG495, OG515, OG530, OG550, OG570, and OG590—were investigated by means of low-wave-number Raman scattering. The numbers next to the letters point out the cutoff wavelength of the glasses, which is given by both the composition and the size of particles. Two laser excitation lines were used. The krypton ion laser line at 647 nm was used for the Raman excitation providing off-resonance excitation conditions. The spectra were recorded with a Spex 1403 double monochromator equipped with a multichannel detection system (CCD camera Photometrics RDS 900). For the resonance conditions the 514.5-nm line of an argon ion laser and the Dilor Z-24 triple-monochromator Raman spectrometer with a photomultiplier detection unit were used. All Raman spectra were recorded at room temperature using a 90° scattering geometry. The laser power of 300 mW of the krypton ion laser was focused to a spot of 30 μm in diameter. For the resonance condition special care was taken to avoid local heating by using a cylindrical lens for focusing the laser excitation beam on to the sample. The dimension of the laser line focus was 2.6 ×0.03 mm^2 with an applied laser power of 0.3 W, resulting in an excitation power density of 400 W/cm^2. Before recording the Raman spectra, the samples were exposed to the same laser power for 1 h, which leads to a photodarkening of the samples. Such a photodarkened sample is more favorable for detecting Raman-scattered light due to a strong decrease of photoluminescence that usually masks the weak Raman signal. The spectra were taken in VV and HV polarization geometry (the excitation light vertically or horizontally polarized and the scattering light vertically analyzed with respect to the scattering plane).

III. RESULTS AND DISCUSSION

The spectra of acoustical vibrations of a free homogeneous elastic spherical particle contains two types of modes—spheroidal and torsional[15] ones. The modes are classified according to the symmetry group of a sphere by the indices l and m analogous to the harmonic functions Y_{lm}. The symmetric $l=0$ spheroidal modes are purely radial with spherical symmetry. The values $l>0$ measure the number of wavelengths along a circle on the surface. A third index ($p = 1,2,...,n$) labels the sequence of eigenmodes, in increasing order of wave number and radial wave vector, for fixed angular shape (l,m). Duval has shown[16] that for a spherical particle only the spheroidal modes labeled $l=0$ (symmetric) and $l=2$ (quadrupolar) are Raman active. Since the symmetric mode is polarized and quadrupolar depolarized, the depolarization ratio I_{HV}/I_{VV} allows one to decide which mode is Raman active. The wave numbers of these modes—i.e., the lowest-energy mode of the $l=0, 2$ sequences—are given by

$$\tilde{\nu} = \frac{S_l v}{cD}, \tag{1}$$

where $\tilde{\nu}$ is the wave number value in cm^{-1}, v is the longitudinal ($l=0$) and transverse ($l=2$) sound velocity, c is the light velocity, and D is the diameter of the particle expressed in cm. S_l is a proportionality coefficient depending on the angular momentum l, the harmonic number n, and the ratio between the longitudinal and transverse sound velocities, v_L/v_T. Montagna and Dusi[15] calculated the value of this coefficient as a function of v_L/v_T. The results are presented in Fig. 1 of their paper[15] in the form of dimensionless wave numbers. Using their approach and the sound velocities $v_L = 4250$ m/s and $v_T = 1860$ m/s for CdS and $v_L = 3690$ m/s and $v_T = 1620$ m/s for CdSe[17] we obtain the values $S_0 = 0.84$ and $S_2 = 0.91$, which are the same for both semiconductors. Sometimes it is more convenient to use the relation $D = \beta/\nu$. We found that $\beta = 1.29 \times 10^{-5}$ for the symmetric mode of CdS and 1.12×10^{-5} for the symmetric mode of CdSe. For the quadrupolar mode the corresponding values are $\beta = 0.52 \times 10^{-5}$ for CdS and 0.46×10^{-5} for CdSe.

To explain the resonantly and off-resonantly excited low-wave-number acoustical modes we propose the following model. The Raman scattering intensity from a system with spatially confined vibrations is generally described by the Shuker-Gammon relation[18]

$$I(\nu,T) = \frac{n(\nu,T)+1}{\nu} C(\nu) g(\nu), \tag{2}$$

where $C(\nu)$ is the light-to-vibration coupling coefficient, $g(\nu)$ is the density of vibrational states, T is the temperature, and $n(\nu,T)+1$ is the Bose-Einstein occupation factor for the Stokes component. For the off-resonant conditions it has been shown, theoretically, that the light-to-vibration coupling coefficient is proportional to the particle diameter,[15] $C(D) \sim D$. This relation was derived for dielectric materials, far from resonance, and is therefore not valid anymore for the

resonant case where the laser excitation should give an intense Raman contribution. Here, the effects of resonance depend on the strength of electron-phonon[6] and plasmon-phonon[19] coupling that increases with reducing the size of the nanoparticles. By reducing the particle diameter these effects should have great influence on $C(D)$. Therefore, the dependence of the coupling constant could be generally expressed as $C(D) \sim D^{-\alpha}$, where $\alpha > 0$.

For Raman scattering on nanoparticles, the density of vibrational states, $g(\nu)$, represents the number of particles that vibrate with that frequency. On the basis of the corresponding relation $g(\beta/\nu) \sim N(D)$, where the constant β depends on the excited mode, the particle size distribution $N(D)$ can be determined by the density of the symmetric or quadrupolar vibrational modes. We used the following particle size distributions to describe $N(D)$:

(a) Lifshitz-Slyozov distribution[20]

$$N(u) = \frac{3^4 e^{(2u/3-1)^{-1}}}{2^{5/3}(u+3)^{7/3}(3/2-u)^{11/3}} \quad \text{for } u<1.5,$$

$$N(u) = 0 \qquad \text{for } u>1.5, \tag{3}$$

where $u = D/D_0$, and

(b) log-normal distribution

$$N(D) = \frac{e^{-0.5[\ln(D/D_0)/\sigma]^2}}{D\sigma\sqrt{\pi/2}}. \tag{4}$$

The Lifshitz-Slyozov distribution describes crystallites grown under conditions of thermodynamic equilibrium with a tail to smaller diameters, and we used this expression for the case when the main contribution to the Raman scattering comes from small particles, $D \ll D_0$, which is the case for the resonant condition. The log-normal distribution is used for off-resonant conditions when the main contribution to the Raman spectra comes from larger particles ($D > D_0$).

For the resonance Raman scattering experiments on particles of a single diameter D, Eq. (2), should be then multiplied with a resonant scattering factor[21]

$$L(D,E_{\text{exc}}) \propto \frac{1}{[E(D)+E_{\text{ph}}-(E_{\text{exc}}+U_{\text{trap}})]^2+\Gamma^2}. \tag{5}$$

Here the laser excitation of energy E_{exc} is in resonance with the coupled particle electronic state $E(D)$ and the vibrational state E_{ph}, respectively. Γ is the linewidth of the HOMO-LUMO (highest occupied and lowest unoccupied molecular orbitals) transition peak. At room temperature, $\Gamma_{\text{hom}} = 0.06$ eV.[22,23] The free excitons are mostly coupled to the long-wavelength optical phonons via the Frühlich interaction. The energy of these phonons is $E_{\text{ph}} = 38$ meV (305 cm^{-1}) for CdS and $E_{\text{ph}} = 26$ meV (210 cm^{-1}) for CdSe. The term U_{trap} in Eq. (5) has been added for the case the excitation starts from a trap level inside the optical gap. The total Raman scattering for the resonance and off-resonance conditions is the integral of the homogeneous broadened Raman spectrum over the inhomogeneous distribution:

$$I(\nu,E_{\text{exc}}) \propto \frac{n(\nu)+1}{\nu} \int C(\nu,D) N(D) L(D) dD. \tag{6}$$
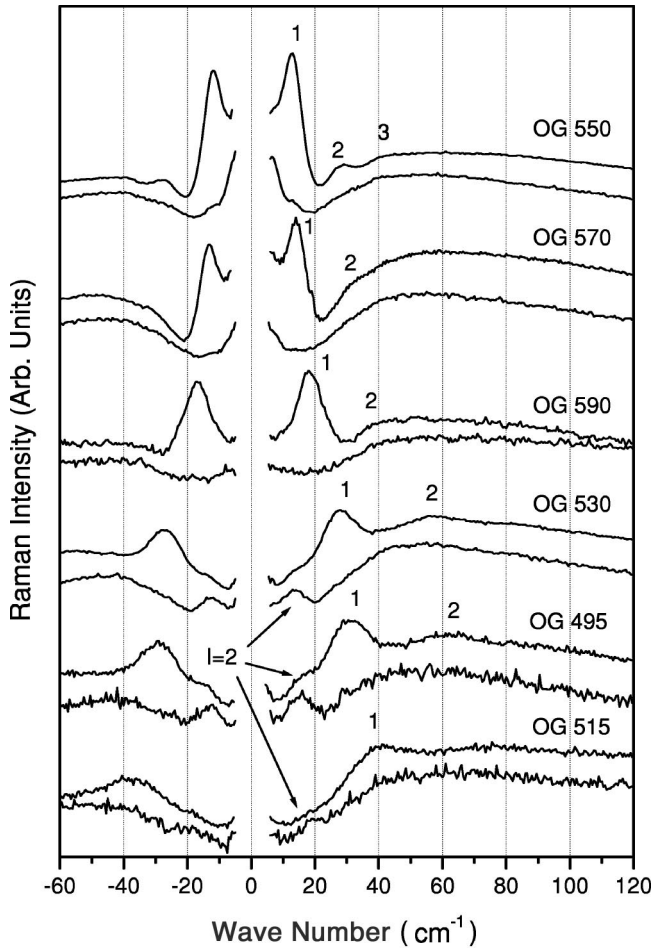
FIG. 1. Low-wave-number VV- (upper) and HV- (botom) po-larized Raman spectra of different Schott glasses (the p sequence of the $l=0$ symmetric mode is labeled). The particle modes are super-imposed onto the broadband-"boson peak" and the quasielastic scattering that correspond to the vibrational excitation of the glass matrix. For the samples with smaller particle diameters (OG 530, OG 515, and GG 495), the $l=2$ mode can be also seen.

A. Off-resonance excitation

Figure 1 shows the low-wave-number VV- and HV-polarized Raman spectra of the acoustical vibrations of CdS_xSe_{1-x} particles. Both types of modes, symmetric and quadrupolar, appear in the polarized VV spectra. Beside the symmetric surface mode ($p=1$), the symmetric inner modes ($p=2,3$) are also observable in the spectra. The quadrupolar mode is depolarized and can be clearly seen in the HV-polarized spectra. For this vibration the inner modes ($p>1$) were not observed. The calculation predicts almost one order of magnitude lower intensity for these modes in comparison to the symmetric ones. This could explain why they are missing in the Raman spectra.[15] All modes are su-perimposed on both the "boson peak" [24]—a broad signal that is a common feature for most glasses having its maxi-mum near $50\ cm^{-1}$—and on the low-energy quasielastic scattering peak[25] (QS) that appears below $30\ cm^{-1}$.

Figure 2 shows the calculated Raman spectra using Eq. (6) and the log-normal distribution for different distribution
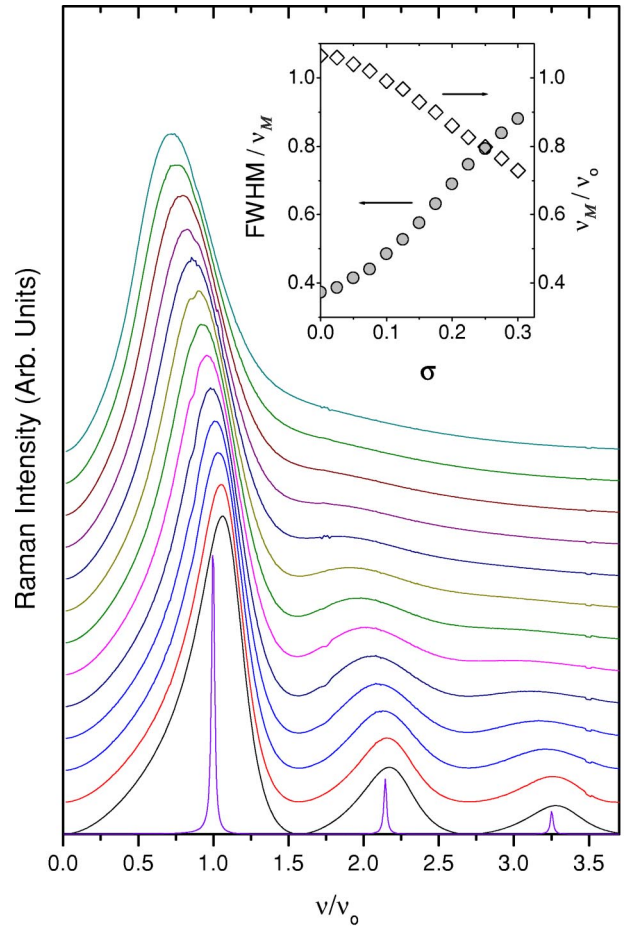
FIG. 2. The effects of the particle size distribution width on the symmetric surface ($p=0$) and symmetric inner modes ($p=2,3,...$). The log-normal function was used for the description of the size distribution. The first narrow spectrum is the calculation for a free nanoparticle. The other spectra from the bottom to the top are homogeneously and inhomogeneously broadened spectra, where the width σ increases from 0 to 0.3 in steps of 0.025. The peak wave numbers ν_M were normalized to the maximum of the symmetric mode ν_0 of the free nanoparticle. The inset shows the influence of the distribution width σ on the symmetric mode peak ν_M and on the normalized full width at half maximum of the symmetric mode, Γ_{FWHM}/ν_M.

widths σ. Since the excitation is far from a resonance, we use $L(D)\sim const$. The calculations were performed on the basis of the Montagna-Dusi approach for the VV Raman spectrum of the symmetric modes (for details see Ref. 15). The param-eters used to calculate the spectra were $v_L=5960$ m/s, $v_T=3790$ m/s for the sound velocities and $\rho=2.3$ g/cm^3 as the density of silica glass, and 4.87 g/cm^3 and 5.66 g/cm^3 for the densities of CdS and CdSe, respectively. The resulting spec-tra show the homogeneously broadened modes caused by the particle interaction with the surrounding medium. For a com-parison the spectrum for a free particle is also presented in Fig. 2. The inset in Fig. 2 shows the influence of the distri-bution width σ on the symmetric mode peak ν_M and on the normalized full width at half maximum of the symmetric mode Γ_{FWHM}/ν_M.

FIG. 3. The I_{VV}-1.8I_{HV} spectra fitted with the boson peak and the CdS$_x$Se$_{1-x}$ symmetric modes inhomogeneous broadened due to particles size distributions. The parameters D_0 and σ are results of the fit.

In order to remove the contribution of the low-wave-number quasielastic scattering, the HV-polarized spectra were divided with the depolarization ratio of QS, which, measured for the samples applied in this studies, is $\rho_{QS} = 5/9$, and then subtracted from the VV-polarized Raman spectra. We note that the quadrupolar mode is depolarized and, therefore, its contribution is mainly cancelled by applying this procedure. The resulted spectra VV-9/5*HV then consists of the $l=0$ symmetric mode, its inner radial modes ($p=2,3,...$), and the rest of the boson peak. Figure 3 shows the VV-1.8*HV Raman spectra together with the fitted boson peak and the CdS$_x$Se$_{1-x}$ symmetric modes. The phenomenological function[26] const$\times \nu^3 (40^2 + \nu^2)^{-1.7}$ was used to fit the boson peak on all spectra. The Raman spectra of the symmetric surface and inner modes were fitted with Eq. (6). The distributions widths σ found from the fit were between 0.15 and 0.175. This agrees with the results of Irmer *et al.*[11] who measured the size distributions of CdS$_x$Se$_{1-x}$ particles in Schott glass using the anomalous small x-ray scattering method. They found sharp distributions of the full width at half maximum of 20%–40% of the mean particle diameters. From the inset of Fig. 2 the inhomogeneous contribution to the linewidth of the symmetric mode can be determined to be $\sim$30%, which is a considerable value. Due to the shift of the symmetric mode with the size distribution width σ, we sug-

gest to use a corrected equation for the determination of the mean particle diameter of the following form:

$$D = \frac{(1.12 + 0.17x) \times 10^{-5}}{\nu_M}(1.12 - 1.31\sigma). \quad (7)$$

Here, ν_M is the maximum wave number value of the observed symmetric mode peak, x is the CdS content, and σ is the distribution width which lies for the Schott glass between 0.15 and 0.175. This relation is valid for $\sigma < 0.3$ and can be of practical interest.

B. Resonance excitation

For the resonance Raman spectra the excitation line is located in the range of the first absorption peak. The Raman spectra contain the resonantly excited zone-center LO-like phonons of CdS at $\sim$300 cm^{-1} and CdSe at $\sim$200 cm^{-1} and their second-order bands as well as the low-wave-number acoustical (particles) modes. The LO-like peaks change their position and intensity for different alloy compositions and can therefore be used to determine the crystalline composition x. On the basis of the wave number difference ν_{dif} between CdS and CdSe LO modes the composition x can be calculated according to[27] $\nu_{dif} = 60 + 55x$ in cm^{-1}. Using this simple relation we found $x=0.81$, 0.51, and 0.71 for GG 595, OG 515, and OG 550, respectively. Figure 4 shows the corresponding photoluminescence (PL) spectra excited with the 514.5-nm laser line. The PL spectra exhibit well-defined peaks due to the band-edge luminescence and peaks caused by carriers recombination on defects.[28] The absence of the band-edge luminescence for the sample GG 495 indicates that the excitation is still below the band gap and, therefore, this sample was near-resonantly excited.

Figure 5 shows the low-wave-number VV and HV Raman spectra excited with 514.5 nm. For a comparison, the spectra excited off resonantly, with 647 nm, are also presented. The near-resonance effect for the OG 495 sample manifests itself in an intensity enhancement and broadening of the symmetric mode in the VV-polarized spectrum. The resonance Raman spectra of the OG 515 sample were taken with an excitation energy equal to the cutoff energy—i.e., just in resonance with the band gap. The two particle peaks are observed under both VV and HV polarization geometry. Their positions are very close to the symmetric and quadrupolar modes observed under off-resonance excitation. The high-energy peak is slightly depolarized in comparison to the symmetric mode observed off resonantly. We ascribe this peak to the polarized symmetric mode. The appearance of the depolarized component could be explained due to a strong multiple elastic scattering of the incident excitation light on nanoparticles. In this case the memory of the incoming light polarization vector could be lost, resulting in the appearance of a depolarized component. The resonance Raman spectrum of the OG 550 sample was taken with an excitation energy much above the band gap. Here also the depolarized component of the observed particle peak appears. Since this peak is far away in wave numbers from the symmetric and quadrupolar mode recorded off resonantly, this case is a nice example for a resonance size selective
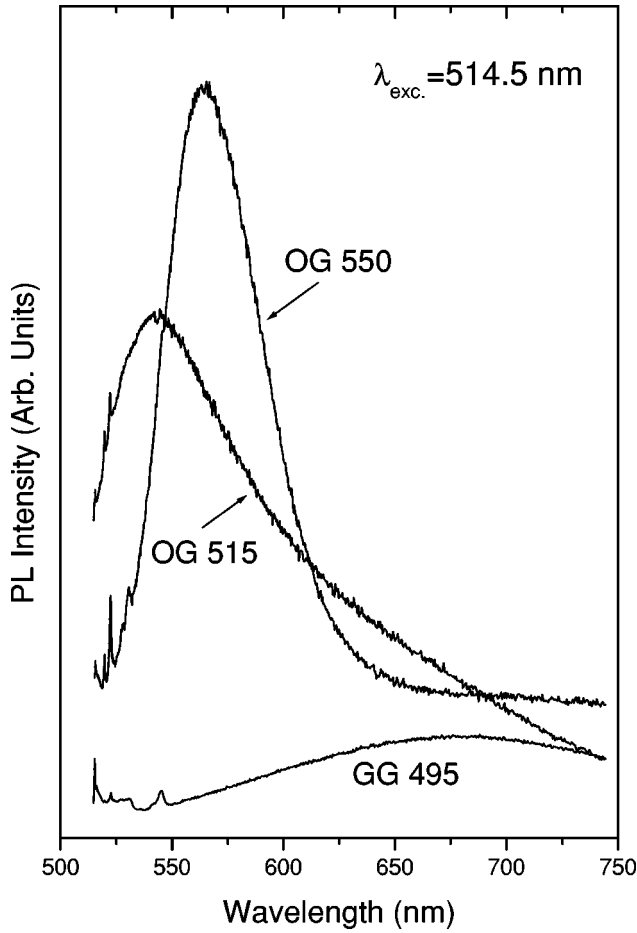
FIG. 4. The photoluminescence spectra of resonantly excited Schott glasses.

excitation of the nanoparticles. This is a clear evidence that in this case the coupling coefficient $C(D)$ in Eq. (6) strongly selects particles of small size, due to a resonance of the laser energy with that of some electronic transition.

To fit the resonance Raman spectra with Eq. (6), we have to know how the LUMO energy level of semiconductor nanoparticle $E(D)$ is shifted with respect to those of bulk. The lowest direct interband transition energy of a spherical quantum dot of diameter D has been obtained by Kayanuma[29] by applying a variational calculation for the band-gap energy of a confined system. In our resonance Raman scattering experiment we expect small particles to be excited and, therefore, we will use the case of strong confinement discussed by Kayanuma.[29] The lowest energy of an electron-hole pair in such a system is given by

$$E(D) = E_0 + \frac{2\hbar^2\pi^2}{\mu D^2} - 3.572\frac{e^2}{\varepsilon D} - 0.248 E_{Ry}^*, \quad (8)$$

where E_0 is the energy gap of the macroscopic crystal, m is the reduced mass, e the electron charge, ε is the high-wave-number dielectric constant of material, and $E_{Ry}^* = (\mu e^4/2\varepsilon\hbar^2)$ is the effective Rydberg energy. The second term of Eq. (8) represents the quantum localization energy. The third and fourth terms correspond to the Coulomb potential and the polarization energy, respectively. Using $m_e = 0.18$, $m_h = 0.6$, $\varepsilon = 6.1$, and $E_0 = 1.86$ eV for CdSe and $m_e = 0.12$, $m_h = 0.4$, $\varepsilon = 5.32$, and $E_0 = 2.53$ eV for CdS, Eq. (8), CdS_xSe_{1-x} can be expressed as

$$E(x,D) = \frac{5.106x + 10.207}{D^2} + \frac{0.127x - 0.989}{D}$$

$$+ 0.6628x + 1.853. \quad (9)$$
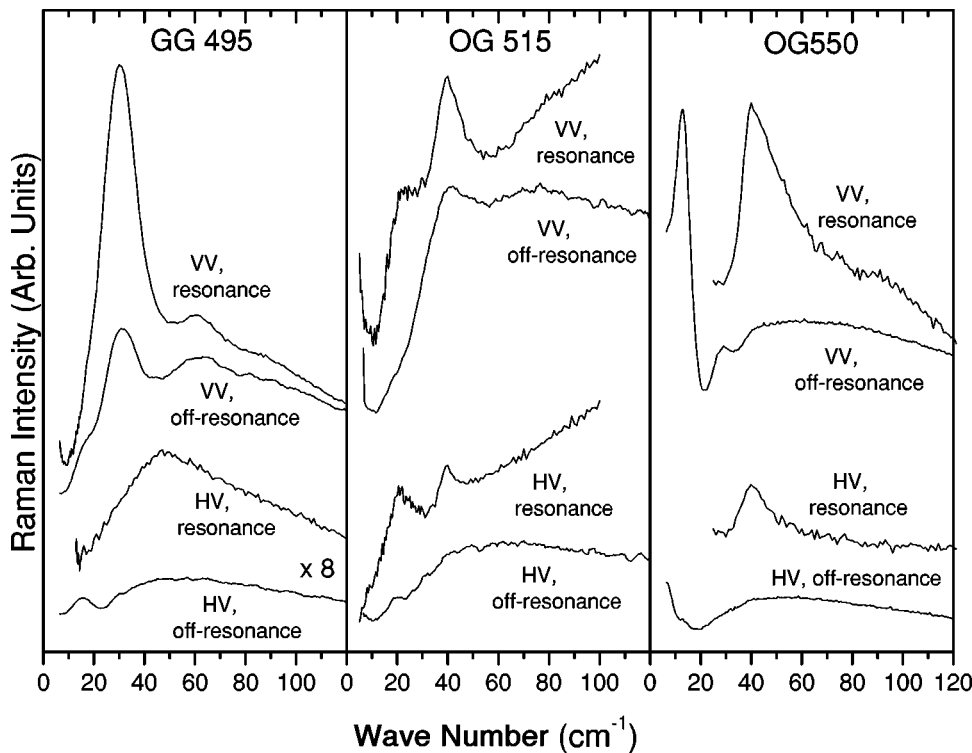
FIG. 5. The low-wave-number resonance Raman spectra of GG 495, OG 515, and OG 550 taken with 514.5 nm laser excitation. For a comparison the off-resonance Raman spectra taken with 647 nm laser excitation are also presented.
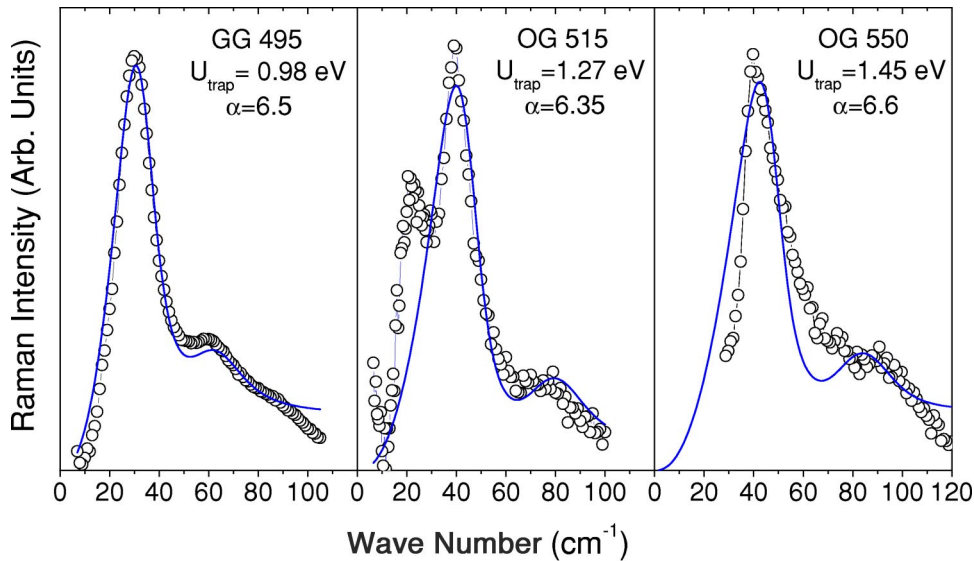
FIG. 6. Raman spectra of resonantly excited particle modes of different samples (circuits). The solid line represents the fit of Eq. (6). The trap energy U_{trap} and the exponent α from the $C(D) \sim D^{-\alpha}$ dependence are results of the fit.

Here E is measured in eV and D in nm. In Eq. (9), we have used a linear interpolation of the physical quantities between $x=0$ and $x=1$. The calculation was performed by taking care of the units in Eq. (8), e^2 was replaced by $e^2/4\pi$, and μ and ε were expressed in the units of the electron mass and dielectric constant of vacuum, respectively.

Figure 6 shows the fit of Eq. (6) on the resonantly excited acoustical modes for different Schott glasses: GG 495, OG 515, and OG 550. The spectra were taken from Fig. 5 (*VV* in-resonance component) applying a linear background subtraction. The fitting parameters were U_{trap}, the exponent α from the $C(D) \sim D^{-\alpha}$ dependence, and the excitonic linewidth Γ. We note that the fit with the homogeneous excitonic width, $\Gamma = 0.06$ eV, gave poor results. The best results were obtained for $\Gamma = 0.25$ eV. This value corresponds to the inhomogeneous excitonic width which indicates that almost all particles from the size distribution assemble were involved in the scattering process.[21] We note that without introducing the trap energy U_{trap} it is not possible to explain the position of the peaks in the resonance Raman spectra. Another interesting result is the values of the exponent α obtained from the fit lying in the range $6 < \alpha < 7$, resulting in a very strong increase of the light-to-vibration coupling coefficient while reducing the particles diameters under resonance excitation conditions.

In Fig. 7 a possible mechanism for the observed phenomena is shown. The laser excites electrons from the HOMO into the LUMO state (process 1). Some of the excited carriers relax via deep trap centres (process 2) and some by direct recombination. The carriers are most likely trapped in the states localized at the semiconductor-matrix interface[30] or outside the nanocrystals in the surrounding matrix.[31] Trapping of carriers outside the nanocrystals has been suggested as a possible origin of the photodarkening effect.[32] When a critical population of the trap states outside the nanocrystals is established by a photodarkening process, the laser light now starts excitations from these states into LUMO states of the neighboring nanocrystals (process 3). Only those crystals with LUMO states that satisfy $E(D_{res}) = E_{exc} + U_{trap}$ will be excited. The excited carriers in these crystals undergo again

the standard relaxation pathways—by direct recombination or capturing by traps (process 4).

C. Comparison with other results

First, we compare our relation for the determination of the crystal size under off-resonance conditions by using the peak wave number value of the symmetric mode. Saviot *et al.*[14] compared the wave numbers of the symmetric mode with the radii of CdS particles. In combination with the data published by Tanaka *et al.*[33] and Othmani[34] they determined β to be 1.31×10^{-5}. Verma *et al.*[13] obtained a similar result $\beta = (1.26 \pm 4) \times 10^{-5}$ comparing Raman, transmission electron microscopy (TEM), and ASAX data. These values agree with the β value we obtained applying Eq. (7) using $x=1$ and $\sigma = 0.15$ ($\beta = 1.19 \times 10^{-5}$).
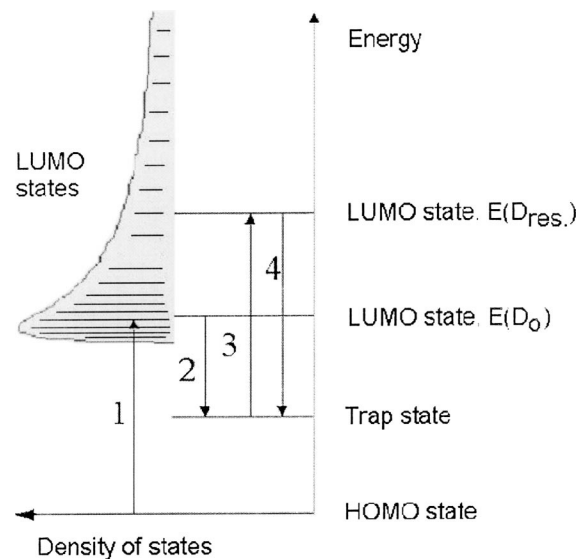
FIG. 7. The proposed mechanism for resonance Raman scattering of photodarkened samples: (1) excitation from HOMO to LUMO, (2) recombination with deep traps, (3) excitation to LUMO starting from trap states, and (4) recombination with deep traps.
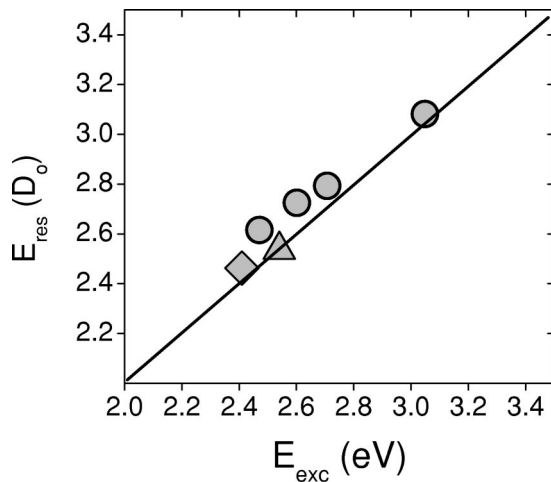
FIG. 8. The correlation of the optical gap calculated from the peak wave number of the resonantly excited symmetric mode width the corresponding laser excitation energy: circles, from Saviot *et al.* (Ref. 14): triangle, Lapinska-Kalita *et al.* (Ref. 8): and diamond, our value.

Second, we have tested the validity of Eq. (8) to determine the energy gap from the known particle diameter D using the resonance Raman scattering data at a low-irradiation level, where the photodarkening process is not significant. Saviot *et al.*[14] excited CdS samples with different laser excitation energies. They used a low-irradiation level to avoid heating and photodarkening effects. Under resonance conditions a new (resonantly excited) peak appears that shifts to higher wave numbers with the laser excitation energies. We took their four most characteristic values. Using the peak wave numbers of the resonantly excited particle ν_0 at a low-irradiation level, we calculate the corresponding mean particle diameters using $D_0 = 1.10 \times 10^{-5}/\nu_0$ and by applying Eq. (9) their optical gap $E_{res}(D_0)$. Figure 8 shows the correlation of $E_{res}(D_0)$ with the excitation energy. We also added onto the graph the value of the lower-energy particle peak recorded by Lipinska-Kalita *et al.*[8] of $CdS_{0.88}Se_{0.12}$ under resonance conditions and at low flux by using 488 nm excitation. Finally, we also present in Fig. 8 our corresponding low-energy peak of the OG 515 shown in Fig. 6. This peak should correspond to the excitation process 1 shown in Fig. 7. All the results presented in Fig. 8 show a good (expected) proportionality between the calculated energy gap of the particles and the excitation energy, proving the validity of Eq. (9).

Finally we have to explain the appearance of the second high-energy peak observed by Saviot *et al.*[14] and Lipinska-Kalita *et al.*[8] for a low-irradiation level. The work presented here shows that this high-energy peak, excited resonantly at high irradiation, corresponds to the process 3 in Fig. 7, which is LUMO excitations from deep traps. We note that this process can also take place at a low laser irradiation, but under strong resonance conditions—i.e., when the excitation energy is in resonance with the majority of the nanoparticles—i.e., with the band-gap energy of the particles from the maximum of the size distribution. In this case the filling of such trap states could be large enough to initiate process 3 shown in Fig. 8, resulting in the appearance of the second peak even at a low-irradiation level.

IV. CONCLUSION

In this paper we have analyzed the low-wave-number Raman scattering from nanosized CdS_xSe_{1-x} crystals embedded in a glass matrix. In the off-resonance scattering regime the spectral shape and width of the symmetric mode was calculated considering the homogeneous (interaction of particles with a matrix) and inhomogeneous broadening (due to particle size distribution) and was compared to the experimental Raman spectra. From the fit, the mean particle size distribution width was determined. A considerable contribution of an inhomogeneous broadening of 30% in linewidth of the symmetric mode was estimated. Under resonance scattering conditions the selective excitation of nanoparticles of photodarkened samples has been analyzed. By comparing the experimental results with a model calculation, we have shown that the ground levels for resonance excitation are trap states filled with the carriers produced by the photodarkening process. The determined trap energies are in the range 1–1.5 eV. On the basis of this phenomenon, the nanoparticles with an optical gap larger than the excitation energy will be possible to excite resonantly. The technique of resonance Raman scattering on acoustical modes could be a new tool for the investigation of the origin and dynamic of the photodarkening process.

*Electronic address: wolfgang.kiefer@mail.uni-wuerzburg.de

[1] G. Bret and F. Gires, Appl. Phys. Lett. **4**, 175 (1964).

[2] R. K. Jain and R. C. Lind, J. Opt. Soc. Am. **73**, 647 (1983).

[3] J. Yumoto, S. Fukuskima, and K. Kubodera, Opt. Lett. **12**, 832 (1987).

[4] C. N. Ironside, T. J. Cullen, B. S. Bhumbra, J. Bell, W. C. Banyai, N. Finlayson, C. T. Seaton, and G. I. Stegeman, J. Opt. Soc. Am. B **5**, 492 (1988).

[5] S. I. Najafi, M. Belanger, R. Maciejko, and R. J. Black, Appl. Opt. **27**, 806 (1988).

[6] S. Schmitt-Rink, D. A. Miller, and D. S. Chemla, Phys. Rev. B **35**, 8113 (1987).

[7] E. Duval, A. Boukenter, and B. Champagnon, Phys. Rev. Lett. **56**, 7052 (1986).

[8] K. E. Lipinska-Kalita, G. Mariotto, and E. Zanghellini, Philos. Mag. B **71**, 547 (1995).

[9] T. Bischof, M. Ivanda, G. Lermann, A. Materny, and W. Kiefer, J. Raman Spectrosc. **27**, 297 (1996).

[10] L. Saviot, B. Champagnon, E. Duval, I. A. Kudriavtsev, and A. I. Ekimov, J. Non-Cryst. Solids **197**, 238 (1996).

[11] G. Irmer, J. Monecke, P. Verma, G. Goerigk, and H. Herms, J. Appl. Phys. **88**, 1873 (2000).

[12] P. Verma, W. Cordts, G. Irmer, and J. Monecke, Phys. Rev. B **60**, 5778 (1999).

[13] P. Verma, L. Gupta, S. C. Abbi, and K. P. Jain, J. Appl. Phys. **88**, 4109 (2000).

[14] L. Saviot, B. Champagnon, E. Duval, and A. I. Ekimov, Phys. Rev. B **57**, 341 (1998).

[15] M. Montagna and R. Dusi, Phys. Rev. B **52**, 10 080 (1995).

[16] E. Duval, Phys. Rev. B **46**, 5795 (1992).

[17] *Semiconductors*, edited by M. Schultz, Landolt-Börnstein, New Series, Vol. 4 (Springer, New York, 1998). The sound velocities were calculated as a mean value for different crystalline directions (1,5,7 for v_L and 2,3,4,5,6 for v_T).

[18] R. Shuker and R. W. Gammon, Phys. Rev. Lett. **25**, 222 (1970).

[19] E. Duval, H. Portes, L. Saviot, M. Fuji, K. Sumitomo, and S. Hayashi, Phys. Rev. B **63**, 75405 (2001).

[20] I. M. Lifshitz and V. V. Slyozov, J. Phys. Chem. Solids **19**, 35 (1961).

[21] A. P. Alivisatos, T. D. Harris, P. J. Carroll, M. L. Steigerwald, and L. E. Brus, J. Chem. Phys. **90**, 3463 (1989).

[22] A. P. Alivisatos, A. L. Harris, N. J. Levinos, M. L. Steigerwald, and L. E. Brus, J. Chem. Phys. **89**, 4001 (1988).

[23] F. Henneberger, J. Puls, Ch. Spiegelber, A. Schülzgen, H. Rossmann, V. Jungnickel, and A. I. Ekimov, Semicond. Sci. Technol. **6**, A41 (1991).

[24] M. Ivanda, W. Kiefer, and G. Mariotto, Solid State Commun. **117**, 423 (2001).

[25] A. Fontana, F. Rossi, G. Carini, C. D'Angelo, G. Tripodo, and A. Bartolotta, Phys. Rev. Lett. **78**, 1078 (1997).

[26] M. Ivanda, Phys. Rev. B **46**, 14 893 (1992).

[27] A. Tu and P. D. Persans, Appl. Phys. Lett. **58**, 1506 (1991).

[28] M. Ivanda, T. Bischof, G. Lermann, A. Materny, and W. Kiefer, J. Appl. Phys. **82**, 3116 (1997).

[29] Y. Kayanuma, Phys. Rev. B **38**, 9797 (1988).

[30] X. Zhang and H. Hamaguchi, Phys. Rev. B **50**, 14 718 (1994).

[31] T. Rajh, O. I. Micic, D. Lawless, and N. Serpone, J. Phys. Chem. **96**, 4633 (1992).

[32] P. Roussignol, D. Ricard, J. Lukasik, and C. Flytzanis, J. Opt. Soc. Am. B **4**, 5 (1987).

[33] A. Tanaka, S. Onari, and T. Arai, Phys. Rev. B **47**, 1237 (1993).

[34] A. Othmani, Ph.D. thesis, Universite Lyon, 1994.